environmental microbiology

Environmental Microbiology (2013) **15**(12), 3252–3258 doi:10.1111/1462-2920.12197

Three-dimensional structure of the Z-ring as a random network of FtsZ filaments

Oreste Piro,[1] Gideon Carmon,[2,3†] Mario Feingold[2,3‡] and Itzhak Fishov[4*,‡]

[1]*Departamento de Física, Universitat de les Illes Balears, E-07122 Palma de Mallorca, Spain.*

[2]*Department of Physics, Ben Gurion University of the Negev, Beer Sheva 84105, Israel.*

[3]*The Ilse Katz Center for Nanotechnology, Ben Gurion University of the Negev, Beer Sheva 84105, Israel.*

[4]*Department of Life Sciences, Ben-Gurion University of the Negev, Beer Sheva 84105, Israel.*

Summary

The spatial organization of the Z-ring, the central element of the bacterial division machinery, is not yet fully understood. Using optical tweezers and subpixel image analysis, we have recently shown that the radial width of the Z-ring in unconstricted *Escherichia coli* is about 100 nm. The relatively large width is consistent with the observations of others. Moreover, simulation of the experimental FtsZ distribution using the theoretical three-dimensional (3D) point spread function was strongly in favour of a toroidal rather than a thin cylindrical model of the Z-ring. Here, we show that the low density of FtsZ filaments in the ring coincides within experimental uncertainty with the critical density of a 3D random network of cylindrical sticks. This suggests that the Z-ring may consist of a percolating network of FtsZ filaments. Several factors that are expected to affect the polymerization state and the extent of self-interaction of FtsZ within the Z-ring, as well as the functional implications of its sparse toroidal structure, are discussed in terms of percolation theory.

Introduction

In bacteria, the cytoskeletal tubulin homologue, FtsZ, is the central structural element of cell division machinery (den Blaauwen *et al.*, 2008). FtsZ polymerized into protofilaments forms a ring centred in the constriction plane and subsequently recruits a series of ~13 additional proteins to this so-called 'Z-ring' (Erickson *et al.*, 2010). However, we still do not understand the three-dimensional (3D) organization of the FtsZ filaments within the Z-ring. It was widely believed that these filaments assemble in a thin layer next to the cytoplasmic membrane (CM) and are mutually co-aligned. In this configuration, FtsZ protofilaments would encircle the membrane surface only two and a half times (Erickson *et al.*, 2010), an estimation that is based on the amount of FtsZ in the cell (about 6000 molecules per cell) and the distribution of fluorescent FtsZ between the ring and cytoplasm (30% and 70%, respectively) (Anderson *et al.*, 2004; Geissler *et al.*, 2007). The view of the Z-ring as a thin layer was inspired by the observations that FtsZ can form bundled filaments in solution and on flat surfaces in a concentration-dependent manner (Erickson *et al.*, 2010) and supported by electron cryotomography of *Caulobacter crescentus* (Li *et al.*, 2007), where the FtsZ concentration was shown to be maximal at 16 nm below the CM. Moreover, Li *et al.* (2007) found only a small number of FtsZ filaments in the Z-ring.

In contrast, Fu *et al.* (2010) used photoactivated localization microscopy (PALM) to image the Z-ring of *Escherichia coli* and observed a significantly wider radial FtsZ distribution than that indicated in Li *et al.* (2007). This led them to propose that the Z-ring is toroidally shaped. We have used optical trapping to align *E. coli* cells with their long axis perpendicular to the imaging plane (Carmon *et al.*, 2012). This approach allowed us to obtain images of the Z-ring that were close to circularly symmetric and measure its radial width, D. We found that $D = 100 \pm 20$ nm. Moreover, our data suggest that the Z-ring image is well approximated by a torus whose minor diameter is D. Subsequently, a 3D PALM study of *C. crescentus* has shown that the corresponding radial width of the Z-ring is between 70 and 100 nm (Biteen *et al.*, 2012), a result that is consistent with ours. The relatively large volume of the Z-ring poses the question of how this torus can be assembled from the small number of FtsZ filaments in the ring.

Discerning between the two structural models is also crucial for our understanding of the Z-ring function. For example, it will shed new light on the question of

Received 8 February, 2013; revised 10 June, 2013; accepted 13 June, 2013. *For correspondence. E-mail fishov@bgu.ac.il; Tel. (+972) 8 646 1368; Fax (+972) 8 646 1710. †Present address: Samsung Electronics UK Ltd, Holland Building, Europark, 60972 Yakum, Israel. ‡These authors have contributed equally to this work.

Z-ring restructuring during constriction and a presumed constriction-associated force generation. In particular, knowing the structure of the Z-ring would allow addressing the question whether force generation occurs as a result of filament sliding along a flat bundle (Lan *et al*., 2009) or via condensation from a sparse to a denser packing in a torus.

Here, we summarize our experimental results and suggest a model that describes the spatial organization of the FtsZ filaments in the wide Z-ring. In particular, we suggest that the density of FtsZ filaments in the Z-ring is consistent with that of a 3D percolating network.

Results

Toroidal structure of the E. coli *Z-ring imaged in optically aligned cells*

Rod-shaped bacteria are traditionally imaged by means of conventional microscopy, while their long axis lies in the focal plane (horizontal alignment). Such imaging can be used to determine the localization and dynamics of different proteins along the cell (Govindarajan *et al*., 2012) or to monitor the evolution of the cell shape during the division cycle (Reshes *et al*., 2008a). Using this approach, we have previously shown that Z-ring positioning occurs at an earlier time, τ_z, than that for the onset of constriction, τ_c (Tsukanov *et al*., 2011).

In addition to the information provided by the horizontal images about the stage of the cell cycle and the distribution of the FtsZ-GFP on the CM, vertical images allow determining whether the formation of the Z-ring has ended, $t > \tau_z$. We found that for $t > \tau_z$, vertical Z-ring images display an almost perfect circular symmetry (see fig. 2 in Carmon *et al*., 2012) and the distance between the ring and the CM can be measured with high accuracy. The first step in our analysis consists of finding the centres of symmetry for the images of both the CM and the Z-ring. In the second step of the analysis, we compute the intensity levels along radial rays emerging from the centre of symmetry. Moreover, averaging the 360 radial profiles for each of the circularly symmetric images led to a smooth function, the average radial profile, *I(r)*. The *I(r)* profile describes the fluorescence intensity variation along the radial direction. We found that the maximum of the CM average radial profile is farther from the cell axis than the corresponding maximum of the Z-ring. The difference between the radii of the two maxima, Δr, is ~50 nm (see fig. 3a in Carmon *et al*., 2012). Because the outermost layer of the Z-ring is attached to the CM via FtsA and ZipA proteins (Adams and Errington, 2009), we proposed that Δr corresponds to half the radial width of the Z-ring, *D*. Further support for this relation was obtained from the analysis of the geometry of the cellular structures that correspond to the observed images. We have used the 3D point spread function to model the image of the different possible object geometries and compared the model images with those obtained from experiment.

First, to mimic the FtsZ distribution observed by Li *et al*. (2007), we considered a cell model where the Z-ring is represented by a cylindrical surface that coincides with the CM, centred at midcell and extending 100 nm along the cell axis. Extracting the average integral profiles from the model images and locating their respective maxima, we obtained $\Delta r = 12$ nm (see fig. 3b in Carmon *et al*., 2012), much smaller than the measured Δr. This suggests that our measurements are not compatible with the cylindrical model and the findings of Li *et al*. (2007).

To reproduce the value of Δr measured in our experiment, a second cell model was simulated with a toroidal Z-ring located at mid-cell and with a radial width of 100 nm. Using this model, we obtained $\Delta r = 48$ nm (see fig. 3c in Carmon *et al*., 2012) in good agreement with our experimental results. We propose that this agreement between the toroidal model and experiment represents strong evidence that the proposed relation between the distance between the maxima of the CM and FtsZ *I(r)*'s and the radial width of the Z-ring, $D \approx 2\Delta r$, holds within the range of our experimental error.

In order to turn the toroidal Z-ring hypothesis into a fully self-consistent model, we need to resolve the puzzle as to how do the few FtsZ filaments assemble to fill up the relatively wide ring. No simple answer to this question can be found if one accepts the widespread view that the FtsZ filaments are at least partially co-aligned. However, here, we show that the number of FtsZ filaments available closely corresponds to the density necessary to form a randomly aligned network. Such networks have been extensively analysed in the framework of percolation theory.

Percolation model for the 3D structure of the Z-ring

Percolation models were first introduced by Broadbent and Hammersley (1957). In their work, percolation was used to describe the process whereby fluid penetrates an immersed rock and to inquire whether it may reach its centre. Aside from rock permeability, percolation has been used to model connectivity and transport in a wide variety of disordered systems (Stauffer and Aharony, 1991).

In the framework of percolation theory, the critical density necessary to form connected networks has been determined for elements of various geometries. In what follows, we employ results for the continuum percolation of rod-like objects (Balberg *et al*., 1984a,b) to estimate this density for a network of FtsZ filaments. Specifically, we model these filaments as long cylindrical rods that are randomly assembled within the Z-ring with random relative orientations. The critical density, ρ_c, is defined as the

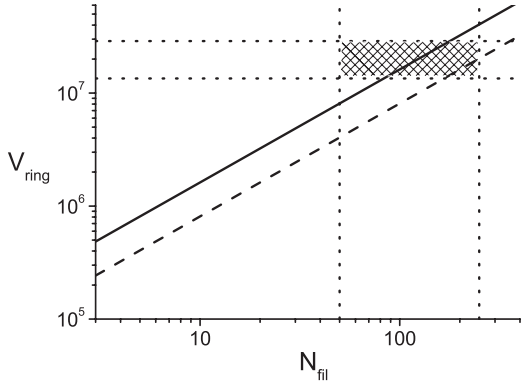

Fig. 1. Phase diagram of the Z-ring. While the range of experimental error in the Z-ring volume, V_{ring}, lies between the horizontal dotted lines, the range in the number of FtsZ filaments in the ring, N_{fil}, consistent with the different measurements is between the vertical dotted lines. Therefore, the cross-hatched rectangle represents the region of experimental uncertainty. The solid and the dashed lines represent the percolation thresholds for the capped cylinders networks modeling the configurations with and without ZapA bridges, respectively.

number of such rods per unit volume necessary to obtain a connected network. Using a combination of geometrical analysis and Monte-Carlo simulations, Balberg *et al.* (1984a,b) showed that:

$$\rho_c \approx \frac{0.89}{dL^2} \tag{1}$$

for rods of length L and diameter d ($L >> d$). Equation 1 is obtained from the expression for the excluded volume of randomly oriented cylinders capped with hemispheres in the limit where $L >> d$ (see Experimental procedures for details). FtsZ protofilaments are on average 120 nm long (Chen and Erickson, 2005; Erickson *et al.*, 2010) and 5 nm wide (Li *et al.*, 2007) corresponding to a critical density $\rho_c \approx 1.2{\cdot}10^{-5}$ nm^{-3}. As will be shown later, this value of ρ_c falls within the range of filament densities in the toroidal Z-ring, ρ_0, stemming from our measurements of the radial width of the torus and the currently accepted estimates on the total quantity of FtsZ in *E. coli*.

To estimate ρ_0,we need to evaluate the number of FtsZ filaments in the Z-ring, N_{fil}, and the volume of the ring, V_{ring}. N_{fil} is determined by the total number of FtsZ molecules per cell, N_{cell}, the fraction of these molecules that belong to the Z-ring, f_{ring}, and the average number of molecules per FtsZ filament, M, $N_{fil} = N_{cell} \cdot f_{ring}/M$. N_{fil} was calculated using the values of N_{cell}, f_{ring} and M reported in the literature, as described in the *Experimental procedures* section. The uncertainty in the ring volume, V_{ring}, was obtained from our measurements for the Z-ring dimensions (Carmon *et al.*, 2012) and the cell radius (Reshes *et al.*, 2008a,b). The result of these estimates (see Experimental procedures) is that the value of ρ_0 is between $1.7{\cdot}10^{-6}$ nm^{-3} and $1.9{\cdot}10^{-5}$ nm^{-3}. We note that this range marginally includes the value of ρ_c.

In Fig. 1, we show the phase diagram of V_{ring} and N_{fil}. While the cross-hatched rectangle represents the region of experimental uncertainty, a given density corresponds on this diagram to a straight line of unit slope. Thus, the range of ρ_0 that is compatible with the existing measurements is scanned by the lines of slope one that intersect the uncertainty rectangle. In addition, the dashed line represents the value of ρ_c as obtained from Eq. 1. In the phase diagram of Fig. 1, a continuous network of FtsZ filaments is possible in the region below the ρ_c line. Because the lower right corner of the uncertainty rectangle lies below the ρ_c line, it is natural to conclude that there is a good chance that the Z-ring in *E. coli* consists of a continuous random network of FtsZ protofilaments. Moreover, the fact that the ρ_c line intersects the uncertainty rectangle may indicate that the formation of the Z-ring coincides with the percolation event.

The model that leads to Eq. 1 assumes that in the percolating network the capped cylinders are in direct contact with each other. In other words, each object is in contact with at least one other object. However, in the Z-ring, the network of FtsZ filaments is apparently cross-linked by ZapA protein bridges. ZapA is found as a tetramer (Mohammadi *et al.*, 2009), and its length of about 10 nm was obtained from the crystal structure of its *Pseudomonas aeruginosa* homologue (Low *et al.*, 2004). The effect of the ZapA bridges can be included in the capped cylinder model via an enhanced effective width, d_{eff}. Each of the contact bridges is equally shared by two of the filaments in the network. Moreover, the bridges can be attached anywhere on the surface of a filament. Therefore, assuming the ZapA bridges to be perpendicular to the FtsZ filaments, we may estimate the increase in the width of the effective capped cylinders in the percolation model by the extent of the bridge length, $d_{eff} \approx d + 10$ nm. This corresponds to an aspect ratio of 0.125 still within the range of validity of Eq. 1 (see *Experimental procedures*), leading to a reduced critical density, $\rho_c = 0.4{\cdot}10^{-5}$ nm^{-3}. This lower value of ρ_c lies near the centre of the experimental uncertainty rectangle (see Fig. 1) such that our model predicts the presence of a percolating network of FtsZ filaments for about half of the range of Z-ring densities.

In the light of the considerations in the previous paragraph, it is natural to presume that the FtsZ filaments in the Z-ring are assembled in a random network with a density that, within experimental uncertainty, is equal to the percolation threshold. This description of the Z-ring organization allows for the small number of FtsZ filaments available to fill the large toroidal volume of the Z-ring that was observed in recent experiments. Moreover, it is also possible that the formation of the Z-ring coincides with the percolation of the FtsZ filaments.

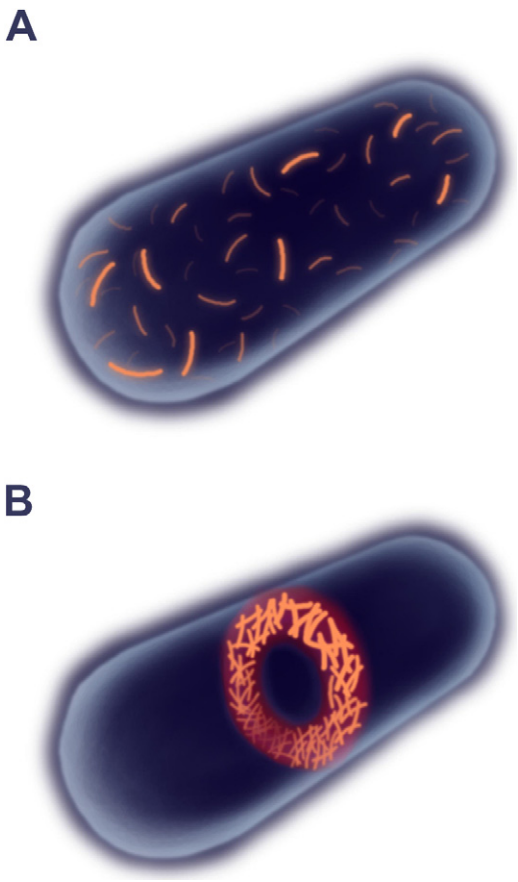

Fig. 2. Schematic view of the Z-ring assembly.
A. Before the formation of the Z-ring, FtsZ filaments (depicted in red) are randomly distributed throughout the cytoplasm and the CM.
B. An interconnected random network of FtsZ filaments form a wide toroidal Z-ring at midcell. For simplicity, the FtsZ that is outside the Z-ring is not shown.

Finally, we discuss the main simplifying assumptions of our analysis. First, the results in Balberg *et al.* (1984a,b) were obtained for an infinite system and do not depend on its overall shape. It is not clear to what extent these apply to the case of the Z-ring where only about 100 filaments assemble in a torus of slightly smaller width, D, than their average length, L. Nevertheless, for the case of spheres Monte-Carlo simulations showed that using only 100 spheres lowers the value of ρ_c by only ~20% (Balberg *et al.*, 1984a). Changes of this order are small relative to the effect of the ZapA bridges that modifies ρ_c by ~70% (Fig. 1). Second, while the length of the FtsZ filaments is widely distributed (Erickson *et al.*, 2010), the percolation model we use assumes a fixed length for the capped cylinders. However, there is evidence that ρ_c does not change when the fixed length of the objects is replaced with a random distribution. This was explicitly shown by Monte-Carlo simulations in thwo-dimensional for circles and widthless sticks and in 3D for spheres (Balberg *et al.*, 1984b). Third, it was suggested that there are no ZapA bridges in the newly formed Z-ring, and these only consolidate the ring after it has formed (Mohammadi *et al.*, 2009). Because with or without the contribution of the ZapA bridges the corresponding ρ_c line intersects the experimental uncertainty rectangle (Fig. 1), the scenario proposed in Mohammadi *et al.* (2009) is consistent with our percolating network model for the structure of the Z-ring.

Discussion

Aligned imaging of the Z-ring lying in the focal plane (Carmon *et al.*, 2012) and other techniques (Fu *et al.*, 2010; Biteen *et al.*, 2012) have revealed its extended structure from the CM towards the cell centre. Our quantitative measurements of the corresponding fluorescence distribution are compatible with a toroidal model for the Z-ring of a ~100 nm width. To understand the structure of a Z-ring of such geometry, one needs to keep in mind two additional considerations: (i) there is a limited number of FtsZ protofilaments available in the cell, and (ii) the ring should be anchored to the CM. Because a configuration of bundled FtsZ filaments adjacent to the CM contradicts the wide radial FtsZ distribution, we propose instead that these filaments are assembled in a random percolating network. In this network, the FtsZ filaments are located at random positions within the toroidal Z-ring, each of them is randomly oriented and in direct contact with at least one other neighbouring filament (see Fig. 2B). Our hypothesis is further supported by the observation that FtsZ filaments form an elastic gel structure *in vitro* for a wide range of concentrations including those in live cells (Esue *et al.*, 2005; Dajkovic *et al.*, 2010).

Although recent experimental evidence indicates that the Z-ring extends away from the CM far into the cytoplasm rather than being ribbon-shaped, it is worthwhile considering the possibility of a random assembly of FtsZ filaments within a thin band adjacent to the CM. Such configuration can be described using the same rod percolation model presented in the previous section. For example, the density for the same amount of FtsZ filaments in a ribbon of 30 nm width (Li *et al.*, 2007) is about 10 times higher than that of a toroidal Z-ring. Assuming the same critical density as before (see Eq. 1), the larger density ensures that a random network of FtsZ filaments will be percolating throughout the entire range of possible *in vivo* concentrations. Therefore, the rod percolation model that we have analysed applies to both the toroidal model for the Z-ring and that of a thin ribbon. However, here, its purpose is to examine the consistency of the toroidal model.

The validity of our model for the structure of the Z-ring as a percolation network is assessed by comparing the

experimentally estimated density of FtsZ filaments in the ring with the value of the percolation critical density, ρ_c (Eq. 1). As shown in Fig. 1, the density of FtsZ filaments in physiological conditions can reach or exceed the critical value required for the formation of a random network. While the twofold uncertainty in the Z-ring volume is due to the experimental error in the width of the toroidal region, the fivefold range in the number of FtsZ filaments reflects the widely different values of the intracellular FtsZ concentration reported in the literature (summarized in table 1 in Erickson *et al*., 2010).

It is worthwhile noting that the critical density of Eq. 1 depends on the length of the FtsZ filaments, *L*, the value of which was obtained from electron microscopy *in vitro* measurements of *E. coli* FtsZ (Chen and Erickson, 2005; Erickson *et al*., 2010). Larger values of *L* were also obtained using dynamic measurements (Reija *et al*., 2011), which would imply that a large fraction of the uncertainty domain of Fig. 1 would enable the formation of a continuous network. On one hand, the *in vitro* value of *L* might differ from the physiological length of the filaments that has not yet been determined in *E. coli*. On the other hand, within the Z-ring ZapA can promote polymerization and stabilize the filaments (Dajkovic *et al*., 2010), thus further enhancing their effective length.

In addition to the effect of ZapA, several other factors are expected to affect the polymerization state and the extent of self-interaction (bundling) of FtsZ. For example, *in vitro* macromolecular crowding facilitated the formation of longer FtsZ filaments and ribbons but did not change the critical concentration of FtsZ for oligomerization (Gonzalez *et al*., 2003; Reija *et al*., 2011). The larger effective length and width of the interacting rods will lower the value of the critical density (see Eq. 1) and therefore increase the probability for the formation of a percolating network of FtsZ filaments in the Z-ring. In contrast, binding of the soluble part of ZipA, sZipA, to FtsZ did not alter the self-association equilibrium between FtsZ monomers (Martos *et al*., 2010). Another important factor, namely, the anchoring of the Z-ring to the membrane via ZipA and FtsA, may determine the spatial organization of the FtsZ filaments in the suggested toroidal structure. Specifically, a filament that is bound to the CM by more than a single linker protein is unlikely to be randomly oriented in 3D. However, it was shown that *in vitro* one sZipA molecule binds to one FtsZ filament of at least six monomers length (Martos *et al*., 2010). This binding stoichiometry is consistent with the *in vivo* concentration ratio of FtsZ to ZipA and to the other anchoring protein, FtsA, [about 5:1(Rueda *et al*., 2003)] and does not preclude the possibility that the binding site of an FtsZ filament to the membrane is most likely located at one of its ends.

Another implicit assumption in our description of the Z-ring structure is that the FtsZ filaments form a static network. However, it was shown that there is fast turnover of the FtsZ monomers between the Z-ring and cytoplasmic pool (Stricker *et al*., 2002). The direct effect of this turnover is the polymerization and depolymerization of the FtsZ filaments in the ring that in turn affects the filament length polydispersity and its spatial distribution. Nevertheless, as already mentioned in the previous section, the value of the critical density was shown to depend only on the average filament length and not on their distribution (Balberg *et al*., 1984b; Chatterjee, 2010). This suggests that the dynamics of the Z-ring should not affect the predictions of our model.

In view of the Z-ring structure emerging from our network model, it is worthwhile to consider its functional implications. First, one may expect that the previously observed sudden stabilization of the Z-ring at mid-cell (Tsukanov *et al*., 2011) is associated with the phase transition to the gel state upon reaching critical density of FtsZ filaments. Such scenario would provide the necessary framework for a quantitative model of Z-ring formation. Second, the presence of a wide structure at mid-cell might constitute an obstacle for the diffusion of proteins between the two cell halves. However, the occupied volume fraction of our random network is particularly low between 0.6% and 2.9%, such that it appears to have a negligible effect on intracellular diffusion relative to that because of bulk macromolecular crowding in the cytoplasm (Kumar *et al*., 2010). Finally, we may extend our model to the constricting Z-ring using the dynamics of the septal width (Reshes *et al*., 2008a), and the finding that the total number of FtsZ monomers in the Z-ring remains approximately constant during constriction (Lan *et al*., 2009). Assuming that the radial width of the Z-ring, *D*, does not change or may even decrease during constriction, the filament density in the constricting ring is expected to grow. Quite generally, in percolation models the average number of bonds per object is proportional to the density of objects (Balberg *et al*., 1984b). For our random network, this implies an increased number of bonds between the FtsZ filaments and, consequently, a more robust structure of the smaller ring. Accordingly, the growing energy of interaction between the filaments within the Z-ring is expected to promote the advance of the constriction. Although this scenario seems plausible, further analytical and numerical analysis of our model for this case is limited by the lack of sufficient information on the ring composition and dimensions during constriction.

To conclude, the existing experimental data provide support for a sparse toroidal rather than a thin ribbon structure of the Z-ring. Moreover, our model of a connected random network of FtsZ filaments can plausibly describe such structure. This concept may require revisiting our view on the structure of the Z-ring, its dynamics and interaction with the other divisome proteins.

Experimental procedures

Percolation of randomly oriented rods

To provide insight on the possible relation between the structure of the incipient Z-ring and that of a percolating network, we follow the approach suggested by Balberg *et al*. (1984b). For randomly aligned cylinders of length L and diameter d that are capped with hemispheres, it was shown using Monte-Carlo simulations that ρ_c is inversely proportional to the corresponding average excluded volume of the object, $<V_{ex}>$. The excluded volume of an object, O, is defined as the volume enclosed by the surface described by the centre of a second identical object, O', as it slides along the surface of O maintaining at least one point of contact and its 3D orientation. For random alignment, $<V_{ex}>$ is averaged over the relative 3D angle between O and O'. Moreover, the product $<V_{ex}>\cdot\rho_c$ gives the excluded volume of the entire system at the critical density, <V>. For objects that are parallel to each other, $<V>$ is an approximate dimensional invariant, namely, only varies by about 10% for the different object shapes that were studied. Specifically, for a system of parallel objects enclosed in a unit square, $<V> \approx 3$, and for spheres of radius r ($r << 1$), $<V> = 2.8$. However, this feature is lost for non-parallel object systems. For the capped cylinders system:

$$\langle V_{ex} \rangle = \frac{4\pi}{3} d^3 + 2\pi d^2 L + \frac{\pi}{2} dL^2 \qquad (2)$$

In the limit $L >> d$, the last term of Eq. 2 is dominant, and Monte-Carlo simulations give $<V> \cong 1.4$, leading to Eq. 1. Assuming the shape of FtsZ filaments to be well approximated by capped cylinders allows obtaining the corresponding ρ_c. We note however that for the FtsZ filaments the size of the second term in Eq. S1 is about 17% of the value of the third term. Nevertheless, the simulation results of Balberg *et al*. (1984a) show that Eq. 1 is valid up to aspect ratios, d/L, of about 0.25 where the last two terms of Eq. S1 are about the same size. Therefore, the accuracy of Eq. 1 in this range of aspect ratios is better than 2% (the error of the fit in Fig. 1 of Balberg *et al*., 1984a).

Estimating the density of FtsZ filaments in the Z-ring

The total number of FtsZ molecules per cell, N_{cell}, reported for *E. coli* were between 4000 and 15 000 molecules per cell (Erickson *et al*., 2010). Moreover, the partition of FtsZ between the Z-ring and the cytoplasmic pool was estimated (Anderson *et al*., 2004; Geissler *et al*., 2007) yielding f_{ring} between 30% and 40%. This distribution was measured by quantitative fluorescence imaging of cells expressing FtsZ-GFP on the background of native FtsZ. The number of monomers per FtsZ filament, M, corresponds to the ratio between the average filament length and the size of the FtsZ monomer (~ 5 nm), leading to $M \approx 24$. Combining these results, we obtain that the number of filaments in the Z-ring, N_{fil}, is between 50 and 250. The uncertainty in the ring volume, V_{ring}, is due to the measurement error of its radial width. Using the value of the cell radius $R = 466$ nm (Reshes *et al*., 2008a,b), we obtain that V_{ring} is between 1.3×10^7 and 2.9×10^7 nm^3.

Acknowledgements

We thank R. Granek for useful discussions and E. Regev for help with the artwork. This research was supported in part by the Israel Academy of Science and Humanities (Grant no. 1544/08) and the Ministry of Economics and Competitivity of Spain (Grant FIS2010-22322-C02-01 'DAVID').

References

Adams, D.W., and Errington, J. (2009) Bacterial cell division: assembly, maintenance and disassembly of the Z ring. *Nat Rev Microbiol* **7:** 642–653.

Anderson, D.E., Gueiros-Filho, F.J., and Erickson, H.P. (2004) Assembly dynamics of FtsZ rings in Bacillus subtilis and *Escherichia coli* and effects of FtsZ-regulating proteins. *J Bacteriol* **186:** 5775–5781.

Balberg, I., Binenbaum, N., and Wagner, N. (1984a) Percolation thresholds in the three-dimensional sticks system. *Phys Rev Lett* **52:** 1465–1468.

Balberg, I., Anderson, C.H., Alexander, S., and Wagner, N. (1984b) Excluded volume and its relation to the onset of percolation. *Phys Rev B* **30:** 3933–3943.

Biteen, J.S., Goley, E.D., Shapiro, L., and Moerner, W.E. (2012) Three-dimensional super-resolution imaging of the midplane protein FtsZ in live *Caulobacter crescentus* cells using astigmatism. *Chemphyschem* **13:** 1007–1012.

den Blaauwen, T., de Pedro, M.A., Nguyen-Disteche, M., and Ayala, J.A. (2008) Morphogenesis of rod-shaped sacculi. *FEMS Microbiol Rev* **32:** 321–344.

Broadbent, S., and Hammersley, J. (1957) Percolation processes I. Crystals and mazes. *Proc Camb Philol Soc* **53:** 629–641.

Carmon, G., Fishov, I., and Feingold, M. (2012) Oriented imaging of 3D subcellular structures in bacterial cells using optical tweezers. *Opt Lett* **37:** 440–442.

Chatterjee, A.P. (2010) Connectedness percolation in polydisperse rod systems: a modified Bethe lattice approach. *J Chem Phys* **132:** 224905.

Chen, Y., and Erickson, H.P. (2005) Rapid in vitro assembly dynamics and subunit turnover of FtsZ demonstrated by fluorescence resonance energy transfer. *J Biol Chem* **280:** 22549–22554.

Dajkovic, A., Pichoff, S., Lutkenhaus, J., and Wirtz, D. (2010) Cross-linking FtsZ polymers into coherent Z rings. *Mol Microbiol* **78:** 651–668.

Erickson, H.P., Anderson, D.E., and Osawa, M. (2010) FtsZ in bacterial cytokinesis: cytoskeleton and force generator all in one. *Microbiol Mol Biol Rev* **74:** 504–528.

Esue, O., Tseng, Y., and Wirtz, D. (2005) The rapid onset of elasticity during the assembly of the bacterial cell-division protein FtsZ. *Biochem Biophys Res Commun* **333:** 508–516.

Fu, G., Huang, T., Buss, J., Coltharp, C., Hensel, Z., and Xiao, J. (2010) In vivo structure of the *E. coli* FtsZ-ring revealed by photoactivated localization microscopy (PALM). *PLoS One* **5:** e12682.

Geissler, B., Shiomi, D., and Margolin, W. (2007) The ftsA* gain-of-function allele of *Escherichia coli* and its effects on the stability and dynamics of the Z ring. *Microbiology* **153:** 814–825.

Gonzalez, J.M., Jimenez, M., Velez, M., Mingorance, J., Andreu, J.M., Vicente, M., and Rivas, G. (2003) Essential cell division protein FtsZ assembles into one monomer-thick ribbons under conditions resembling the crowded intracellular environment. *J Biol Chem* **278:** 37664–37671.

Govindarajan, S., Nevo-Dinur, K., and Amster-Choder, O. (2012) Compartmentalization and spatiotemporal organization of macromolecules in bacteria. *FEMS Microbiol Rev* **36:** 1005–1022.

Kumar, M., Mommer, M.S., and Sourjik, V. (2010) Mobility of cytoplasmic, membrane, and DNA-binding proteins in *Escherichia coli*. *Biophys J* **98:** 552–559.

Lan, G., Daniels, B.R., Dobrowsky, T.M., Wirtz, D., and Sun, S.X. (2009) Condensation of FtsZ filaments can drive bacterial cell division. *Proc Natl Acad Sci U S A* **106:** 121–126.

Li, Z., Trimble, M.J., Brun, Y.V., and Jensen, G.J. (2007) The structure of FtsZ filaments in vivo suggests a force-generating role in cell division. *EMBO J* **26:** 4694–4708.

Low, H.H., Moncrieffe, M.C., and Lowe, J. (2004) The crystal structure of ZapA and its modulation of FtsZ polymerisation. *J Mol Biol* **341:** 839–852.

Martos, A., Alfonso, C., Lopez-Navajas, P., Ahijado-Guzmn, R., Mingorance, J., Minton, A.P., and Rivas, G. (2010) Characterization of self-association and heteroassociation of bacterial cell division proteins FtsZ and ZipA in solution by composition gradient-static light scattering. *Biochemistry* **49:** 10780–10787.

Mohammadi, T., Ploeger, G.E., Verheul, J., Comvalius, A.D., Martos, A., Alfonso, C., *et al*. (2009) The GTPase activity of *Escherichia coli* FtsZ determines the magnitude of the FtsZ polymer bundling by ZapA in vitro. *Biochemistry* **48:** 11056–11066.

Reija, B., Monterroso, B., Jimenez, M., Vicente, M., Rivas, G., and Zorrilla, S. (2011) Development of a homogeneous fluorescence anisotropy assay to monitor and measure FtsZ assembly in solution. *Anal Biochem* **418:** 89–96.

Reshes, G., Vanounou, S., Fishov, I., and Feingold, M. (2008a) Cell shape dynamics in *Escherichia coli*. *Biophys J* **94:** 251–264.

Reshes, G., Vanounou, S., Fishov, I., and Feingold, M. (2008b) Timing the start of division in *E. coli*: a single-cell study. *Phys Biol* **5:** 046001.

Rueda, S., Vicente, M., and Mingorance, J. (2003) Concentration and assembly of the division ring proteins FtsZ, FtsA, and ZipA during the *Escherichia coli* cell cycle. *J Bacteriol* **185:** 3344–3351.

Stauffer, D., and Aharony, A. (1991) *Introduction to Percolation Theory*. Philadelphia, PA: Taylor & Francis.

Stricker, J., Maddox, P., Salmon, E.D., and Erickson, H.P. (2002) Rapid assembly dynamics of the *Escherichia coli* FtsZ-ring demonstrated by fluorescence recovery after photobleaching. *Proc Natl Acad Sci USA* **99:** 3171–3175.

Tsukanov, R., Reshes, G., Carmon, G., Fischer-Friedrich, E., Gov, N.S., Fishov, I., and Feingold, M. (2011) Timing of Z-ring localization in *Escherichia coli*. *Phys Biol* **8:** 066003.